Reaction Null-Space Control of Flexible Structure Mounted Manipulator Systems

Dragomir N. Nenchev, *Member, IEEE,* Kazuya Yoshida, *Member, IEEE,* Prasert Vichitkulsawat, and Masaru Uchiyama, *Member, IEEE*

***Abstract*—A composite control law for end-effector path tracking with a flexible structure mounted manipulator system is proposed, such that no disturbances on the flexible base are induced. The control law is based on the reaction null space concept introduced earlier to tackle dynamic interaction problems of free-floating robots, or moving base robots in general. The control law is called composite since it ensures base vibration suppression control as well, although independently of the reactionless motion control subtask. The requirement of task independence is essential to avoid the appearance of complex dynamics expressions in the control law, such as nonlinear velocity-dependent coupling terms and dependencies of inertias on the elastic coordinates.**

We present experimental data from computer simulations and the experimental test bed TREP developed at Tohoku university. The experimental data is shown to agree well with theory.

***Index Terms*—Flexible structure mounted manipulator system, reaction null space control, vibration suppression control.**

I. Introduction

THE concept of a so-called *macro-micro manipulator system* was introduced by Sharon and Hardt [1]. A small, high-bandwidth manipulator was mounted on the end of a larger one, and the former was controlled to compensate inaccuracy due to the latter. This concept has evolved throughout the years to meet mainly two types of application demands: nuclear waste cleanup [2], [3] and space robotics [4], [5]. We shall refer to such manipulator systems as *flexible structure mounted manipulator systems*, or FSMS in short.

The control of an FSMS is quite challenging due to complex dynamics, and the presence of dynamic coupling between the two substructures in particular. Such coupling exists regardless of whether the macro part is set in motion or kept stationary. The former case is clearly the more difficult one [6]–[8]. In the latter case, the macro subsystem can be modeled as a passive flexible structure. The motivation behind this case is that, usually, the large arm is actively controlled only when relocating the small arm. Once located at the work site, the small arm is controlled to perform a dextrous operation. Thereby, it may induce some undesirable disturbance in the large passive arm [9]. This latter case will be discussed herein.

Literature survey shows that for single-arm FSMS three main control subtasks can be identified: (1) base vibration suppression control [9]–[12], (2) design of control inputs that induce minimum vibrations[1] [13], and (3) end-point control in the presence of vibrations [14], [15]. A major conclusion is that till now, control subtasks have been tackled mostly separately. Only recently attempts are being made to combine control subtasks into one controller with improved performance. One example is the work of Cannon *et al.* [13], where control subtasks (1) and (2) were combined. Another example is the work of Hanson and Tolson [16]. The authors discuss the important problem of end-point control in combination with vibration suppression control. It should be noted that this task can be solved only when redundancy is present. Hanson and Tolson introduce therefore a kinematically redundant micro part. Vibration suppression control is derived from the null space of the manipulator Jacobian.

The main aim of this work is to propose a composite control law capable of solving all of the three control subtasks above. This composite control makes use of an approximated inverse dynamics model. The approximation reduces computational cost and real-time control becomes feasible despite the complex nature of the problem. Note that real-time is an important issue because the main control mode of FSMS is teleoperation. In spite of the approximation, our approach remains general enough to cover not only single-arm FSMS but also FSMS's with multiple dextrous arms. Such systems we consider important because they enable a control strategy which can be based on so-called *dynamic redundancy*. As already explained, by necessity, we have to consider the presence of redundancy. Kinematic redundancy is one candidate, however, it might not always be a good solution to the problem at hand. Note that kinematic redundancy resolution techniques suffer from the presence of algorithmic singularities. The work of Hanson and Tolson demonstrates this fact. On the other hand, dynamic redundancy is ensured by incorporating actively controlled dynamic parameters, such as inertias and link centroid locations [7]. Such type of control can be obtained via proper arm motion control of FSMS's with multiple dextrous arms [5].

The main contribution of the present work is the combination of two methods developed earlier for free-flying

Manuscript received April 27, 1998; revised February 2, 1999. This paper was recommended for publication by Associate Editor W. Wilson and Editor S. Salcudean upon evaluation of the reviewers' comments. This work was supported by the Ippan C Research Project 07805027 Grand-in-Aid for Scientific Research, Ministry of Education, Science, and Culture, Japan.

D. N. Nenchev is with the Department of Intelligent Machines and System Engineering, Hirosaki University, Hirosaki 036-8561, Japan.

K. Yoshida and M. Uchiyama are with the Department of Aeronautics and Space Engineering, Graduate School of Engineering, Tohoku University, Sendai 980-8579, Japan.

P. Vichitkulsawat is with T. Napa A. Muang, Chonburi 20000, Thailand.

Publisher Item Identifier S 1042-296X(99)10415-4.

[1] We will refer to this subtask also as "reactionless (end-effector) path tracking."

space robot control and for flexible-link manipulator control. First, we will show that the technique for reactionless motion planning [18], [19] and control [20] of a free-flying space robot, referred to as the *reaction null space* approach, is well suited to the problem at hand. Via the reaction null space approach we provide a solution to the second control subtask identified above. Thereafter, within the same framework, we introduce a vibration suppression control law (control subtask one) similar to that used for vibration suppression in flexible-link manipulators [21]. Finally, we show how to extend the formulation to cover also the third control subtask.

The paper is organized as follows. Section II introduces notation and gives some background on the vibration suppression control approach for flexible link manipulators of Konno *et al.* [21] and the reaction null space approach [22]. In Section III, we show how the concept of reaction null space relates to FSMS. Section IV introduces two control laws for base vibration suppression. Section V discusses reactionless end-effector path tracking control. Sections VI and VII present experimental data from a computer simulation and from the experimental setup TREP at Tohoku university, respectively. Finally, the conclusions are given in Section VIII.

II. Notation and Background

A. Equation of Motion

We consider a manipulator arm consisting of n joints. The *system dynamics* can be written in the following form, see e.g. [9]:

$$\begin{bmatrix} \boldsymbol{H}_b & \boldsymbol{H}_{bm} \\ \boldsymbol{H}_{bm}^T & \boldsymbol{H}_m \end{bmatrix} \begin{bmatrix} \ddot{\boldsymbol{x}}_b \\ \ddot{\boldsymbol{\theta}} \end{bmatrix} + \begin{bmatrix} \boldsymbol{D}_b & \boldsymbol{0} \\ \boldsymbol{0} & \boldsymbol{D}_m \end{bmatrix} \begin{bmatrix} \dot{\boldsymbol{x}}_b \\ \dot{\boldsymbol{\theta}} \end{bmatrix} + \begin{bmatrix} \boldsymbol{K}_b \boldsymbol{x}_b \\ \boldsymbol{0} \end{bmatrix} + \begin{bmatrix} \boldsymbol{c}_b \\ \boldsymbol{c}_m \end{bmatrix} = \begin{bmatrix} \boldsymbol{0} \\ \boldsymbol{\tau} \end{bmatrix} \tag{1}$$

where $\boldsymbol{x}_b \in \Re^m$ denotes the positional and orientational deflection of the base with respect to the inertial frame[2], $\boldsymbol{\theta} \in \Re^n$ stands for the joint coordinates of the arm, $\boldsymbol{H}_b(\boldsymbol{x}_b, \boldsymbol{\theta})$, $\boldsymbol{D}_b$ and $\boldsymbol{K}_b \in \Re^{m \times m}$ denote base inertia, damping and stiffness, respectively. $\boldsymbol{H}_m(\boldsymbol{x}_b, \boldsymbol{\theta}) \in \Re^{n \times n}$ is the inertia matrix of the arm. $\boldsymbol{H}_{bm}(\boldsymbol{x}_b, \boldsymbol{\theta}) \in \Re^{m \times n}$ denotes the so-called *inertia coupling matrix*. $\boldsymbol{c}_b(\boldsymbol{x}_b, \dot{\boldsymbol{x}}_b, \boldsymbol{\theta}, \dot{\boldsymbol{\theta}})$ and $\boldsymbol{c}_m(\boldsymbol{x}_b, \dot{\boldsymbol{x}}_b, \boldsymbol{\theta}, \dot{\boldsymbol{\theta}})$ are velocity-dependent nonlinear terms, $\boldsymbol{D}_m$ denotes arm joint damping and $\boldsymbol{\tau} \in \Re^n$ is the joint torque. We do not consider external forces here, including the gravity force, having in mind a noncontact task in micro gravity environment. We note, however, that the micro gravity assumption should not be regarded as a restriction upon the scope of the method introduced herein. Gravity terms can be included into the above equation of motion. A respective compensating term in the control laws below would then account for the presence of gravity, without invalidating the results.

We will now briefly overview two existing techniques to be used as a base in further derivations. One of them is the flexible-link manipulator active vibration suppression technique of Konno *et al.* [21]. The other one is based on the reaction null space approach to a moving base robot [22]. These techniques have been independently developed, each one using a different assumption to approximate the complex dynamics.

[2] Fixed at the equilibrium position/orientation. Generally, $m = 6$ $(n \geq m)$.

B. The Vibration Suppression Control Subtask

The vibration suppression control subtask has been solved by Lee and Book [9] based on the singular perturbation technique. Another possible approach is that of Konno *et al.* used for active vibration suppression of a flexible-link manipulator [21]. At this point, we should note that the equation of motion of a flexible-link manipulator has exactly the same structure as (1) above. The difference is that the flexible coordinates of the FSMS are concentrated at the base, while those of the flexible-link manipulator are distributed over the kinematic chain [23].

The essential assumptions in the work of Konno *et al* are two:

1) since the arm is stationary at the initial instant, the nonlinear velocity-dependent terms $\boldsymbol{c}_b$ and $\boldsymbol{c}_m$ are approximated with zero
2) the deflections are assumed small, and hence, all inertia submatrices are approximated to be functions of the joint variables only.

Note that, also in the case of an FSMS, these two assumptions are sufficient to cancel all velocity-dependent terms, including those which do not contain the joint velocity explicitly (i.e., $\dot{\boldsymbol{H}}_b(\boldsymbol{\theta})\dot{\boldsymbol{x}}_b$, $\dot{\boldsymbol{H}}_{bm}^T(\boldsymbol{\theta})\dot{\boldsymbol{x}}_b$). Then, the upper part of the equation of motion can be linearized around the equilibrium of the base

$$\boldsymbol{H}_b \ddot{\boldsymbol{x}}_b + \boldsymbol{K}_b \boldsymbol{x}_b = -\boldsymbol{H}_{bm} \ddot{\boldsymbol{\theta}}. \tag{2}$$

Without loss of generality, here and henceforth we may ignore base damping. Choosing the control acceleration as

$$\ddot{\boldsymbol{\theta}} = \boldsymbol{H}_{bm}^{+} \boldsymbol{H}_b \boldsymbol{G}_b \dot{\boldsymbol{x}}_b \tag{3}$$

where $\boldsymbol{G}_b$ is a constant gain matrix, $\boldsymbol{H}_{bm}^{+} \in \Re^{n \times m}$ denotes the right pseudoinverse of the inertia coupling matrix[3], and noting that $\boldsymbol{H}_{bm}\boldsymbol{H}_{bm}^{+} = \boldsymbol{E}$, $\boldsymbol{E}$ being an unit matrix of proper dimension, we obtain a damped vibrational system.

C. Reactionless Motion Control Subtask

The assumption regarding a stationary initial state of the manipulator is essential in view of a flexible-link manipulator, where the number of elastic coordinates is usually larger than the number of actuators (in our terms, $m > n$). Now, let us consider the opposite case: a system comprising more actuators than elastic degrees of freedom. In this case we can relax the constraint for stationary initial configuration. The reason is as follows.

At $t = t_0$ we assume a stationary base $(\boldsymbol{x}_b = \boldsymbol{0})$. Then, we look for motions in the micro part which would maintain the zero state of the base. Since the base is stationary, again, all inertia submatrices will be functions of the joint variables only.

[3] The right pseudoinverse can be used, since $n \geq m$ and $\boldsymbol{H}_{bm}$ is assumed full rank. Note, for a flexible-link manipulator the number of elastic coordinates is larger than the number of actuators (in our terms $m > n$), and hence, the left pseudoinverse has to be employed [21].

In addition, all nonlinear velocity-dependent terms contributed by the base deflection rate $\dot{\boldsymbol{x}}_b$ will be zero.

With a stationary base as initial condition, the base reaction wrench $\mathcal{F}_0 = \mathcal{F}(t_0)$ due to motion of the arm can be written as

$$\mathcal{F}_0 = \frac{d}{dt}\left[\boldsymbol{r}_{cm} \times \overbrace{w\dot{\boldsymbol{r}}_{cm} + \sum_{j=1}^{n}(\boldsymbol{I}_j\boldsymbol{\omega}_j + \boldsymbol{r}_j \times m_j\dot{\boldsymbol{r}}_j)}^{w\dot{\boldsymbol{r}}_{cm}}\right] \tag{4}$$

where $\boldsymbol{r}_{cm}$ denotes the position of the total center of mass of the arm, $\boldsymbol{I}_j$, $\boldsymbol{\omega}_j$, m_j, $\boldsymbol{r}_j$ stand for the inertia matrix, angular velocity, mass and center-of-mass position for link j, respectively, and $w = \sum m_j$. The base reaction can be rewritten in terms of arm joint variables, as follows:

$$\mathcal{F}_0 = \boldsymbol{H}_{bm}\ddot{\boldsymbol{\theta}} + \dot{\boldsymbol{H}}_{bm}\dot{\boldsymbol{\theta}}. \tag{5}$$

The state of stationary base will be maintained under a manipulator control law, if it exists, such that $\mathcal{F}(t) = \mathbf{0}$ for all $t \geq t_0$. In this case, base equilibrium is

$$\boldsymbol{H}_b\ddot{\boldsymbol{x}}_b + \boldsymbol{K}_b\boldsymbol{x}_b = \mathbf{0} = -\boldsymbol{H}_{bm}\ddot{\boldsymbol{\theta}} - \dot{\boldsymbol{H}}_{bm}\dot{\boldsymbol{\theta}}. \tag{6}$$

Note the difference when compared with the result from the previous subsection: the term $-\dot{\boldsymbol{H}}_{bm}\dot{\boldsymbol{\theta}}$ does not appear in (2) because of the assumption of stationary initial configuration. Our further derivation will be based on the last equation since the main assumption here is $n > m$.

The specific motion of the manipulator that maintains base equilibrium, i.e.

$$\boldsymbol{H}_{bm}\ddot{\boldsymbol{\theta}} + \dot{\boldsymbol{H}}_{bm}\dot{\boldsymbol{\theta}} = \mathbf{0} \tag{7}$$

we call *reactionless manipulator motion*. The above equation can be integrated to

$$\mathcal{L}(t) = -\mathcal{L}_0 + \boldsymbol{H}_{bm}\dot{\boldsymbol{\theta}}(t), \qquad t \geq t_0 \tag{8}$$

where $\mathcal{L}_0 = \mathcal{L}(t_0) = \boldsymbol{H}_{bm}\dot{\boldsymbol{\theta}}(t_0)$ is the integration constant. This integral has been called *the coupling momentum* [24].

III. The Reaction Null-Space of Flexible Structure Mounted Manipulator Systems

The reaction null space concept has been originally formulated with regard to free-floating space robots [18], [19]. Here we apply the same idea within the framework of FSMS's.

A. The Inverse Problem

We are interested in specific manipulator motion which would induce zero disturbance to the base.

Proposition 1: (*Zero reaction*)

The manipulator does not induce any reactions to the base if and only if the coupling momentum is conserved ($\mathcal{L}(t) =$ const $\Leftrightarrow \mathcal{F}(t) = \mathbf{0}$ for all $t \geq t_0$).

The proof follows from the direct examination of (5) and (8).

The inverse problem is defined as "given the condition of reactionless motion, i.e. zero base reaction (or equivalently, constant coupling momentum), find the joint acceleration (or the joint velocity) which would maintain this condition."

As already pointed out, the assumption that the system at hand has more actuators than elastic degrees of freedom $(n > m)$ plays an important role herein. This is in fact a kinematic redundancy condition, with respect to the base motion task.

Proposition 2: At a manipulator configuration $\tilde{\boldsymbol{\theta}}$ such that rank $\boldsymbol{H}_{bm}(\tilde{\boldsymbol{\theta}}) = \max_\theta$ rank $\boldsymbol{H}_{bm}(\boldsymbol{\theta})$:

1) Zero reaction is achieved with the joint acceleration

$$\ddot{\boldsymbol{\theta}}(t) = -\boldsymbol{H}_{bm}^{+}\dot{\boldsymbol{H}}_{bm}\dot{\boldsymbol{\theta}}(t) + (\boldsymbol{E} - \boldsymbol{H}_{bm}^{+}\boldsymbol{H}_{bm})\boldsymbol{\zeta}(t), \quad t \geq t_0 \tag{9}$$

where $\boldsymbol{\zeta}(t) \in \Re^n$ is arbitrary;

2) The coupling momentum $\mathcal{L}_0$ is conserved with the joint velocity

$$\dot{\boldsymbol{\theta}}(t) = -\boldsymbol{H}_{bm}^{+}\mathcal{L}_0 + (\boldsymbol{E} - \boldsymbol{H}_{bm}^{+}\boldsymbol{H}_{bm})\boldsymbol{\zeta}(t), \qquad t \geq t_0 \tag{10}$$

where $\boldsymbol{\zeta}(t)$ denotes again an arbitrary vector.

Proof: Substituting $\ddot{\boldsymbol{\theta}}_c$ from (9) into (5) and taking into account that under the above rank condition $\boldsymbol{H}_{bm}\boldsymbol{H}_{bm}^{+} = \boldsymbol{E}$, one obtains $\mathcal{F}_0 = \mathbf{0}$ with any initial joint velocity $\dot{\boldsymbol{\theta}}(t_0) \equiv \dot{\boldsymbol{\theta}}_0$, and also $\mathcal{F}(t) = \mathbf{0}$, $t > t_0$. Similarly, substituting $\dot{\boldsymbol{\theta}}_c$ from (10) into $\mathcal{L}(t) = \boldsymbol{H}_{bm}\dot{\boldsymbol{\theta}}(t), t \geq t_0$, one obtains $\mathcal{L} = \mathcal{L}_0$, where the initial velocity is such that $\mathcal{L}_0 = \boldsymbol{H}_{bm}\dot{\boldsymbol{\theta}}_0$. □

The expression $\boldsymbol{P}_{RNS}(\boldsymbol{\theta}) \equiv (\boldsymbol{E} - \boldsymbol{H}_{bm}^{+}\boldsymbol{H}_{bm})$ appearing in both (9) and (10), stands for the projector onto the null space $(\boldsymbol{H}_{bm})$ of the inertia coupling matrix.

Definition 2: The null space of the inertia coupling matrix is called *the reaction null-space of an FSMS*.

From (10) it is apparent that the joint velocity comprises two components: one from the reaction null space, and the other from its orthogonal complement. The reaction null-space component does not contribute to the coupling momentum, and hence, it would yield zero reaction.

Corollary: With zero initial coupling momentum, zero reaction is obtained with the velocity

$$\dot{\boldsymbol{\theta}}_{RNS} = \boldsymbol{P}_{RNS}(\boldsymbol{\theta})\boldsymbol{\zeta}. \tag{11}$$

We are interested in the component $\dot{\boldsymbol{\theta}}_{RNS}$ especially from the standpoint of integrability. At each manipulator configuration $\boldsymbol{\theta}$ the columns of the null space projector $\boldsymbol{P}_{RNS}(\boldsymbol{\theta})$ induce a smooth distribution [25] in joint space. In case of well-conditioned inertial coupling at $\boldsymbol{\theta}$ (i.e. the rank condition for the inertia coupling matrix $\boldsymbol{H}_{bm}$ in Proposition 2 holds), then the distribution is nonsingular. According to Frobenius' theorem, a distribution is completely integrable, if and only if it is involutive. Involutivity can be examined via Lie brackets on the columns of $\boldsymbol{P}_{RNS}$. If such involutivity can be established, then the reaction null space component of the joint velocity will be integrable.

Definition 3: The integral of (11), if it exists, is called *the set of reactionless paths of an FSMS*.

The reactionless paths guarantee decoupling between the base dynamics and the manipulator dynamics. Unfortunately, their existence cannot be always guaranteed. The only case when integrability is guaranteed, is that of a one-dimensional distribution (i.e., $n - m = 1$). Nevertheless, in some important practical cases the system can be recast to fit into this category.

B. Existence of the Reaction Null-Space

A necessary condition for the existence of the reaction null-space is the availability of any of the following features:

1) kinematic redundancy;
2) dynamic redundancy;
3) selective reaction null-space;
4) rank deficiency of the inertia coupling matrix.

We utilized *kinematic redundancy* when deriving the solution in the previous section. Recall the SSRMS/SPDM system as a representative example of this category [5]. On the other hand, we applied the concept of dynamic redundancy [17] to the general problem of moving base robotics and reaction management control [22] in assuming that special devices, called reaction compensators, are present. These devices are used just to control the reaction on the base, similarly to the usage of reaction wheels for satellite attitude control.

There are some applications, such as nuclear waste cleanup FSMS, when the stiffness of the flexible base along some of the generalized coordinates can be sufficiently characterized as high-stiffness while in other directions it would be characterized as low-stiffness. Reactions along the high-stiffness directions do not disturb the base at all. In this case we introduce the *selective reaction null space*. Denote a selection matrix by $\boldsymbol{S} = \text{diag}[s_1, s_2, \cdots, s_6]$, where $s_i = 1$ specifies a Cartesian-space low-stiffness direction, requiring zero base reaction, while $s_i = 0$ otherwise. Then, we denote the selective reaction null space as $\aleph\ (\boldsymbol{S}\boldsymbol{H}_{bm})$. Obviously, dim $\aleph(\boldsymbol{S}\boldsymbol{H}_{bm}) \geq$ dim $\aleph\ (\boldsymbol{H}_{bm})$. Generally, a reaction null space of higher dimension is desirable, since it yields more DOF when planning the reactionless motion.

Finally, the reaction null space will also exist when the inertia coupling matrix $\boldsymbol{H}_{bm}$ is rank deficient. Locations where $\boldsymbol{H}_{bm}$ is rank deficient constitute submanifolds in joint space. Thus, if one wishes to exploit rank deficiency to obtain reactionless motion, proper analysis should be done. This approach, however, would limit accessible areas in workspace, which is not desirable from a practical viewpoint. In our study below, we will therefore consider only the first three cases of reaction null space existence. On the other hand, we note that the inversion algorithms derived in Section III-A ((9) and (10)) utilize the pseudoinverse of the inertia coupling matrix. Since pseudoinversion is sensitive to ill conditioning, care should be taken to avoid neighborhoods of such locations.

Finally, we note that sufficient conditions for the existence of the reaction null-space are related to the problem of design. Detailed analysis of this problem goes beyond the scope of the present work. We note here that increasing the number of degree of freedom (DOF) does not necessarily increase the dimension of the reaction null space. Also, note that motion in some of the DOF's, such as wrist motion for example, may yield quite insignificant inertial coupling. Taking an articulated arm with a distinctive upper/lower elbow arm structure as a typical example (e.g., the SSRMS), it should be apparent that reactionless motion can be obtained within the main arm plane. Reactions due to base rotation (which changes the orientation of the arm plane) are difficult to be compensated under the condition of kinematic redundancy. If one considers additional compensators, such as torque control gyros at the base, then base rotation disturbance is compensable via the dynamic redundancy condition.

IV. Vibration Suppression Control of FSMS

Vibration suppression via inertia coupling is a well-known approach applied to FSMS (cf. e.g. [9]), and flexible-link manipulators [21]. Note that no redundancy (in terms of existence of the (selective) reaction null space) was assumed. As already explained, the presence of such redundancy implies the existence of continuous manipulator motion that does not disturb the equilibrium of the elastic subsystem—base or flexible link structure. Even in case of nonstationary (vibrating) base, we can expect that reactionless motion will have a minimal (though not exactly zero) contribution to the change of the state of the base.

We will propose two control laws for vibration suppression. The first one makes use of the assumptions in Section II-B which have been successfully exploited for vibration suppression of flexible-link manipulators [21]. The second control law will be based on exact cancellation of the nonlinearities.

A. Acceleration-Based Vibration Suppression Control

Recall that when the base vibrates, (9) does not exactly reflect the dynamics; there will be additional coupling due to velocity dependent nonlinear terms and due to base position/attitude dependent change of the inertias. Nevertheless, the assumptions in Section II-B can be used since the base is regarded as a passive structure, eventually vibrating around its equilibrium.

Equation (3) can be directly applied to effectively suppress base vibration when the initial arm configuration is stationary. This control law has to be modified, however, to reflect the presence of redundancy:

Proposition 3: (*Acceleration-based vibration suppression control*)

In the presence of redundancy, the control

$$\ddot{\boldsymbol{\theta}} = \boldsymbol{H}_{bm}^{+}(\boldsymbol{H}_b\boldsymbol{G}_b\dot{\boldsymbol{x}}_b - \dot{\boldsymbol{H}}_{bm}\dot{\boldsymbol{\theta}}) + \boldsymbol{P}_{RNS}\boldsymbol{u} \tag{12}$$

where $\boldsymbol{u}$ is an *arbitrary* control input, ensures optimal (in a least squares sense) vibration suppression control.

Proof: Substituting the above control law into (6), we obtain

$$\ddot{\boldsymbol{x}}_b + \boldsymbol{G}_b\dot{\boldsymbol{x}}_b + \boldsymbol{H}_b^{-1}\boldsymbol{K}_b\boldsymbol{x}_b = \boldsymbol{0} \tag{13}$$

where use has been made of the identity

$$\boldsymbol{H}_{bm}\boldsymbol{P}_{RNS} = \boldsymbol{0}. \tag{14}$$

The last equation shows that with proper choice of the *constant* gain $\boldsymbol{G}_b$ we obtain a damped vibrational system. Optimality in least squares sense follows from the property of the pseudoinverse. □

An important result, following from the above identity, is that the arbitrary control input $\boldsymbol{u}$ has no contribution to the vibration dynamics. Hence, this control is potentially useful for other control tasks. We shall come back to the problem in the following subsection.

Remark 1: As noted in [21], no torque appears explicitly in the control equation. Nevertheless, it was shown that implementation of this control law into a velocity-based closed-loop servo controller is straightforward.

Remark 2: It is well known from studies of kinematically redundant systems that the pseudoinverse induces a nonintegrable distribution. This results in drift in configuration space. When the FSMS does not dissipate energy, vibration suppression would result in nonzero coupling momentum conservation, and hence, constant drift of the manipulator in inertial space. In reality, joint damping always exists (cf. the term $\boldsymbol{D}_m\dot{\boldsymbol{\theta}}$ in (1)), and therefore, the arm would stop after a while. In spite of this, it might be desirable to have control over the joint damping process. Hence, we modify our control law as

$$\ddot{\boldsymbol{\theta}}_v = \boldsymbol{H}_{bm}^{+}(\boldsymbol{H}_b\boldsymbol{G}_b\dot{\boldsymbol{x}}_b - \dot{\boldsymbol{H}}_{bm}\dot{\boldsymbol{\theta}}) + \boldsymbol{P}_{RNS}\boldsymbol{u} - \boldsymbol{G}_m\dot{\boldsymbol{\theta}} \tag{15}$$

where $\boldsymbol{G}_m$ is the joint damping control gain. This is possible, since vibration suppression control may admit superposition of a manipulator joint-space nonlinear control law, provided the gains are selected with special care [9], [21].

B. Torque-Based Vibration Suppression Control

Proposition 4: (*Torque-based vibration suppression control)*

Consider the control law

$$\boldsymbol{\tau} = \tilde{\boldsymbol{G}}\dot{\boldsymbol{x}}_b + \tilde{\boldsymbol{c}} + \boldsymbol{H}_m\boldsymbol{P}_{RNS}\boldsymbol{u} - \boldsymbol{G}_m\dot{\boldsymbol{\theta}} \tag{16}$$

where

$$\begin{aligned}\tilde{\boldsymbol{G}} &= \boldsymbol{H}_m\boldsymbol{H}_{bm}^{+}\boldsymbol{G}_b,\\ \tilde{\boldsymbol{c}} &= \boldsymbol{c}_m - \boldsymbol{H}_m\boldsymbol{H}_{bm}^{+}\boldsymbol{c}_b.\end{aligned}$$

Under well-conditioned inertial coupling, the above control guarantees that system damping is achieved.

Proof: From the system dynamics (1) we eliminate the joint acceleration by solving first the upper part for $\ddot{\boldsymbol{\theta}}$ and then, substituting the result into the lower part. We obtain

$$\boldsymbol{\tau} = \tilde{\boldsymbol{H}}\ddot{\boldsymbol{x}}_b + \tilde{\boldsymbol{D}}\dot{\boldsymbol{x}}_b + \tilde{\boldsymbol{K}}\boldsymbol{x}_b + \boldsymbol{D}_m\dot{\boldsymbol{\theta}} + \tilde{\boldsymbol{c}} + \boldsymbol{H}_m\boldsymbol{P}_{RNS}\boldsymbol{\zeta} \tag{17}$$

where

$$\begin{aligned}\tilde{\boldsymbol{H}} &= \boldsymbol{H}_{bm}^{T} - \boldsymbol{H}_m\boldsymbol{H}_{bm}^{+}\boldsymbol{H}_b,\\ \tilde{\boldsymbol{D}} &= -\boldsymbol{H}_m\boldsymbol{H}_{bm}^{+}\boldsymbol{D}_b, \quad \tilde{\boldsymbol{K}} = -\boldsymbol{H}_m\boldsymbol{H}_{bm}^{+}\boldsymbol{K}_b\end{aligned}.$$

The closed-loop system is given by

$$\begin{aligned}&\tilde{\boldsymbol{H}}\ddot{\boldsymbol{x}}_b + \tilde{\boldsymbol{D}}\dot{\boldsymbol{x}}_b + \tilde{\boldsymbol{K}}\boldsymbol{x}_b + \boldsymbol{D}_m\dot{\boldsymbol{\theta}} + \tilde{\boldsymbol{c}} + \boldsymbol{H}_m\boldsymbol{P}_{RNS}\boldsymbol{\zeta}\\ &\quad \tilde{\boldsymbol{G}}\dot{\boldsymbol{x}}_b + \tilde{\boldsymbol{c}} + \boldsymbol{H}_m\boldsymbol{P}_{RNS}\boldsymbol{u} - \boldsymbol{G}_m\dot{\boldsymbol{\theta}}\end{aligned} \tag{18}$$

or

$$\tilde{\boldsymbol{H}}\ddot{\boldsymbol{x}}_b + (\tilde{\boldsymbol{D}} - \tilde{\boldsymbol{G}})\dot{\boldsymbol{x}}_b + \tilde{\boldsymbol{K}}\boldsymbol{x}_b + \boldsymbol{H}_m\boldsymbol{P}_{RNS}(\boldsymbol{\zeta} - \boldsymbol{u}) = \boldsymbol{0} \tag{19}$$

where we assumed that joint damping has been exactly canceled out with $\boldsymbol{G}_m = -\boldsymbol{D}_m$. Premultiplying first by $\boldsymbol{H}_m^{-1}$ and then by $\boldsymbol{H}_{bm}$, we obtain

$$(\boldsymbol{H}_{bm}\boldsymbol{H}_m^{-1}\boldsymbol{H}_{bm}^{T} - \boldsymbol{H}_b)\ddot{\boldsymbol{x}}_b - (\boldsymbol{D}_b - \boldsymbol{G}_b)\dot{\boldsymbol{x}}_b - \boldsymbol{K}_b\boldsymbol{x}_b = \boldsymbol{0} \tag{20}$$

where use has been of the identity (14). Under well-conditioned inertial coupling, the matrix expression $(\boldsymbol{H}_{bm}\boldsymbol{H}_m^{-1}\boldsymbol{H}_{bm}^{T} - \boldsymbol{H}_b)$ is full rank. Then, with proper choice of the constant gain $\boldsymbol{G}_b$, base vibration will be suppressed. □

Remark 1: The above derivation shows that base vibration can be suppressed even with $\boldsymbol{\zeta} - \boldsymbol{u} \neq \boldsymbol{0}$.

Remark 2: The condition for exact cancellation of joint damping can be relaxed in order to gain controllability over arm drift (cf. the discussion in the preceding subsection).

V. Reactionless End-Effector Motion Control

The main difference between existing vibration suppression controls [9], [21] and our control law (12), is the appearance of the term $\boldsymbol{P}_{RNS}\boldsymbol{u}$ in the latter, and also in the torque-based control law (16). Below, we will show that this term is useful to derive a *reactionless end-effector motion* control law.

First, recall that the set of reactionless motion under the condition of a stationary base, as given in (9), is parameterized by the unknown vector $\boldsymbol{\zeta}$. To determine this vector we employ the end-effector kinematics

$$\ddot{\boldsymbol{x}}_e = \boldsymbol{J}\ddot{\boldsymbol{\theta}} + \dot{\boldsymbol{J}}\dot{\boldsymbol{\theta}} \tag{21}$$

where $\boldsymbol{x}_e \in \Re^p$ denotes task coordinates and $\boldsymbol{J}(\boldsymbol{\theta}) \in \Re^{p\times n}$ is the end-effector Jacobian. We assume that the number of task coordinates is less then the actuators $(p < n)$. Note that the reference frame is at the base. After some formula manipulation, one obtains

$$\ddot{\boldsymbol{\theta}} = -\boldsymbol{H}_{bm}^{+}\dot{\boldsymbol{H}}_{bm}\dot{\boldsymbol{\theta}} + \overline{\boldsymbol{J}}^{+}[\ddot{\boldsymbol{x}}_e - \dot{\boldsymbol{J}}\dot{\boldsymbol{\theta}} + \boldsymbol{J}\boldsymbol{H}_{bm}^{+}\dot{\boldsymbol{H}}_{bm}\dot{\boldsymbol{\theta}}] \tag{22}$$

where $\overline{\boldsymbol{J}} \equiv \boldsymbol{J}\boldsymbol{P}_{RNS}$ is a restricted Jacobian matrix appearing typically in redundancy resolution schemes [26]. It can be shown that $\overline{\boldsymbol{J}}^{+}\boldsymbol{\eta} \in \aleph\,(\boldsymbol{H}_{bm})$, for any $\boldsymbol{\eta}$, and hence, the second term on the right hand side is indeed a reaction null space vector. Thus, we can write

$$\boldsymbol{P}_{RNS}\boldsymbol{\zeta} = \overline{\boldsymbol{J}}^{+}[\ddot{\boldsymbol{x}}_e - \dot{\boldsymbol{J}}\dot{\boldsymbol{\theta}} + \boldsymbol{J}\boldsymbol{H}_{bm}^{+}\dot{\boldsymbol{H}}_{bm}\dot{\boldsymbol{\theta}}]. \tag{23}$$

Consider now the following

Proposition 4: (*Reactionless end-effector motion control)*

Let the control law be given by (16) with

$$\boldsymbol{P}_{RNS}\boldsymbol{u} = \overline{\boldsymbol{J}}^{+}[\ddot{\boldsymbol{x}}_e^{d} + \boldsymbol{G}_d\dot{\boldsymbol{e}}_e + \boldsymbol{G}_p\boldsymbol{e}_e - \dot{\boldsymbol{J}}\dot{\boldsymbol{\theta}} + \boldsymbol{J}\boldsymbol{H}_{bm}^{+}\dot{\boldsymbol{H}}_{bm}\dot{\boldsymbol{\theta}}] \tag{24}$$

where $\boldsymbol{x}_e^d$ is the desired end-effector path, $\boldsymbol{e}_e = \boldsymbol{x}_e^d - \boldsymbol{x}_e$ is the path tracking error and $\boldsymbol{G}_d$ and $\boldsymbol{G}_p$ denote proper gain matrices. With a well-conditioned restricted Jacobian $\overline{\boldsymbol{J}}$, the end-effector error converges to zero asymptotically.

Proof: Substitute (23) and (24) into the closed-loop (19), under the condition of a stationary base, to get

$$\boldsymbol{H}_m\overline{\boldsymbol{J}}^{+}(\ddot{\boldsymbol{e}}_e + \boldsymbol{G}_d\dot{\boldsymbol{e}}_e + \boldsymbol{G}_p\boldsymbol{e}_e) = \boldsymbol{0}. \tag{25}$$

Since both $\boldsymbol{H}_m$ and $\overline{\boldsymbol{J}}$ are full rank, with a proper choice of the gains $\boldsymbol{G}_d$ and $\boldsymbol{G}_p$, the end-effector path tracking error must go to zero, asymptotically. □

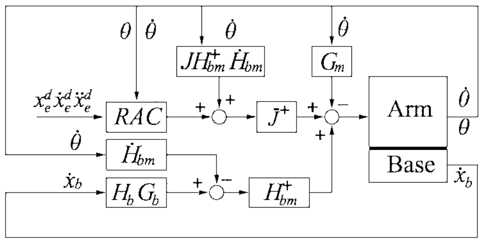

Fig. 1. Acceleration based controller block diagram.

Remark: The full rank condition for the restricted Jacobian $\overline{\boldsymbol{J}}$ implies

1) well-conditioned inertial coupling (since the inertia coupling matrix appears in the formula of this Jacobian);
2) a nonsingular configuration of the manipulator (since the manipulator Jacobian appears in the formula);
3) avoiding any "task conflicts" which are reflected via so-called "algorithmic singularities," well-known from studies on kinematically redundant manipulators.

In summary, we obtained two *composite* control laws, one acceleration based the other torque based, given by (12) and (16) respectively, in combination with (24). The structure of the controllers is essentially the same. Thus, implementations will depend upon the motor drivers at hand. As will be shown below, it is even possible to implement the system within velocity based motor drivers, by approximating appropriately the acceleration based control law. A block diagram for the acceleration based controller is shown in Fig. 1. It is seen that a resolved acceleration controller (RAC) is embedded into the structure. Feedback information is required for joint angles and velocities, and for the flexible base tip deflection (spatial) velocity.

Each of the control laws is capable of, strictly speaking, *either* base vibration suppression *or* reactionless end-effector path tracking (i.e., control subtasks one and two, respectively, as identified in the introduction). As far as the third control subtask is concerned (end-effector control in the presence of vibration), the above derivations show that it can be solved via any of the above schemes, provided there is task sequencing such that end-effector control is initialized only after vibration suppression has been completed. Of course, such task sequencing would introduce additional complexity. Fortunately, the experiments below show that the sequencing can be avoided in practice, and the two subtask can be initialized simultaneously.

VI. Reaction Null Space Via Kinematic Redundancy: Simulation Study

We shall illustrate our approach first with a planar 3R manipulator mounted on a horizontally translating base, which is attached to the inertial frame through a linear spring and a damper. Zero gravity environment is assumed. The parameters of the base are: mass $m_b = 1$ kg, damping $d_b = 0.1$ Nsm^{-1}, stiffness $k_b = 100$ Nm^{-1}. The parameters of the manipulator are: link length $l_i = 1$ m, $(i = 1, 2, 3)$, link mass $m_i = 10$ kg lumped at the center of each link, link moments of inertia have been ignored.

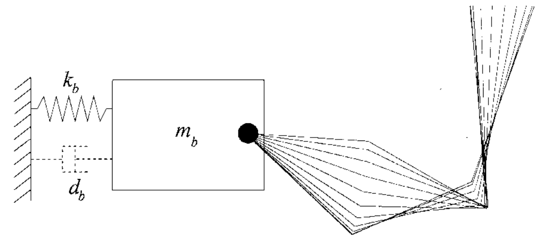

Fig. 2. Model of a kinematically redundant FSMS tracking a reactionless path.

Fig. 2 shows the system, tracking with its end-point a path without inducing any disturbances to the base. Since the reaction null space is 2-D, it is possible to track any path in task space which complies with well-conditioned inertial coupling and full rankness of matrix $\overline{\boldsymbol{J}}$. Because of the decoupling property of the reaction null space, the selection of the feedback gains is not critical: for example, for the end-point control high gains are used ($\boldsymbol{G}_p = \mathrm{diag}[400, 400]$ s^{-2}, $\boldsymbol{G}_d = \mathrm{diag}[200, 200]$ s^{-1}). The gain for base vibration suppression control was $g_b = 10$ rad^{-1}.

First, base vibration suppression is demonstrated. We assume that base vibration is excited due to some external force at $t = 1$ s (see Fig. 3). The base vibrates, with decreasing amplitude because of the natural damping. At $t = 3$ s the vibration control is activated. We have included a joint damping term $-\boldsymbol{G}_m\dot{\boldsymbol{\theta}}$ ($\boldsymbol{G}_m = \mathrm{diag}[1, 1, 1]$ s^{-1}) into the control law for vibration suppression, which guarantees that joint velocity decreases to zero. As already mentioned, if joint damping would not be present, the manipulator would be loaded with a nonzero coupling momentum which is conserved, and which would result in constant drift of the manipulator.

Next, end-effector control is demonstrated. There is no initial deflection of the base. The path is similar to that depicted in Fig. 2, and was planned through a fifth order spline. Other planning can be also used; there is no requirement for zero boundary conditions. Fig. 4 shows the results. The reference path[4] is tracked perfectly, with practically zero base disturbance. Note, that the manipulator comes entirely to rest; no external energy has been introduced into the system which would have caused arm drift.

VII. The Selective Reaction Null Space: Experimental Study

A. Experimental Setup

The experimental setup TREP, designed at Tohoku University, consists of a small 2R rigid link manipulator attached to the free end of a flexible double beam representing a flexible base (Fig. 5). The manipulator is driven by DC servomotors with velocity command input. There is no hardware limit for the rotation of the second joint. In this way, a reactionless path can be tracked in a cyclic manner, and there will be no time limit when performing unidirectional reactionless path tracking

[4] Herein "ref" denotes the reference path, while "act" stands for the actual one.

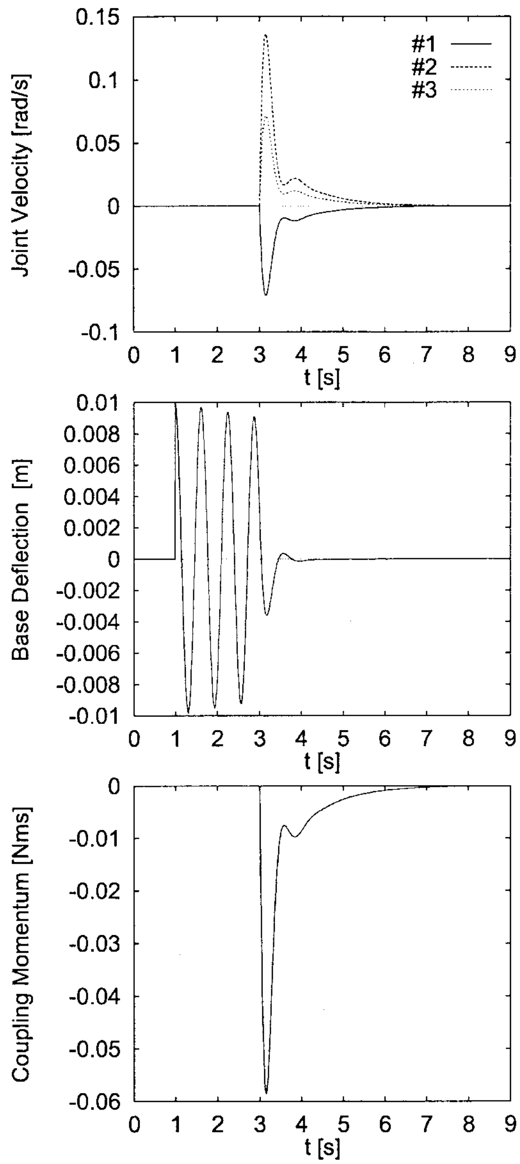

Fig. 3. Kinematically redundant FSMS base vibration control (simulation).

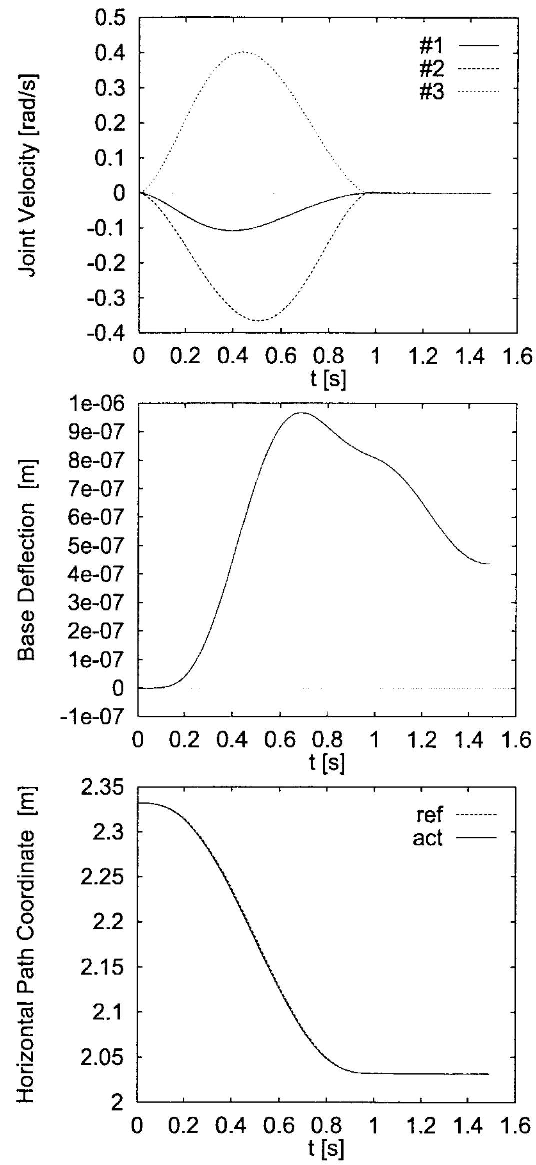

Fig. 4. Kinematically redundant FSMS end-point path tracking (simulation).

experiments. Joint positions are measured by optical encoders and are fed back for position control. Elastic base deflection and base reactions are measured by the strain gauge and the force/torque sensor, respectively. Using a simple static model of the elastic beam, base deflection is transformed into base tip displacement, which is fed back in the control part responsible for base vibration suppression. The photo of TREP is shown in Fig. 6.

B. System Model

The TREP FSMS is modeled according to Fig. 7. The local coordinate frame fixed at the attachment point of the manipulator to the beam, is referred to as the flexible base coordinate frame. The parameters of the manipulator and the base are presented in Tables I and II, respectively. Since the flexible base has been designed as a double beam, the reaction torque can be neglected as a disturbance. This is also the case with the reaction force component along the

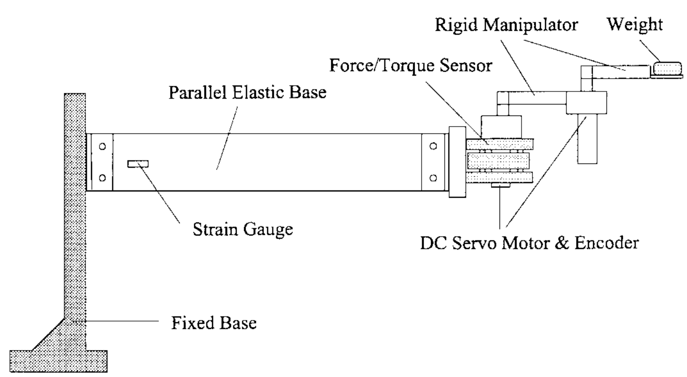

Fig. 5. The experimental FSMS TREP.

longitudinal axis of the base. Thus, we shall consider just the reaction force along the so-called low stiffness direction, which coincides with the x axis of the flexible base coordinate frame. This means that $m = 1$. Since the manipulator has two

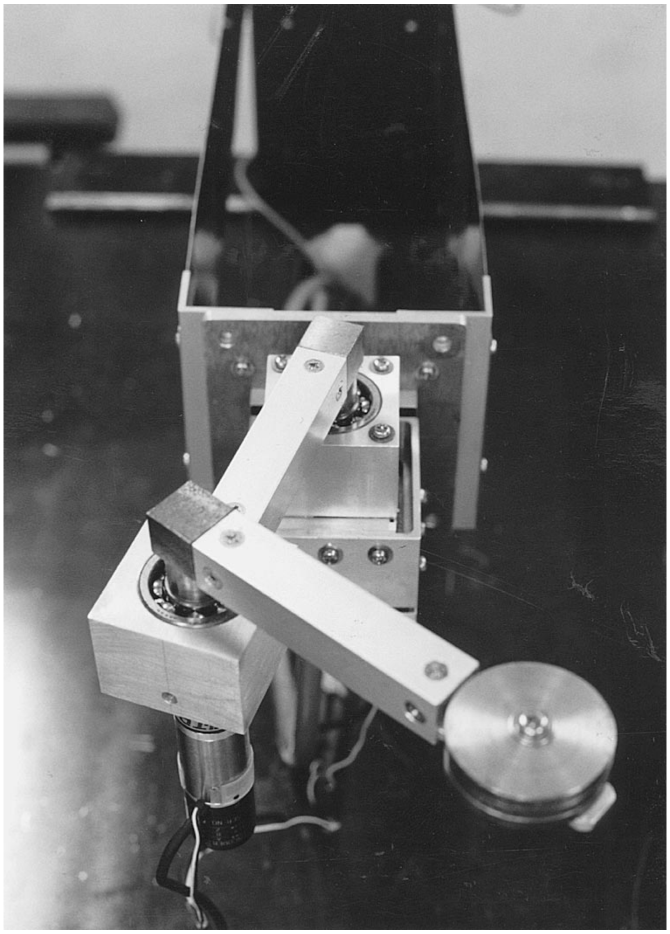

Fig. 6. A photo of the experimental FSMS TREP.

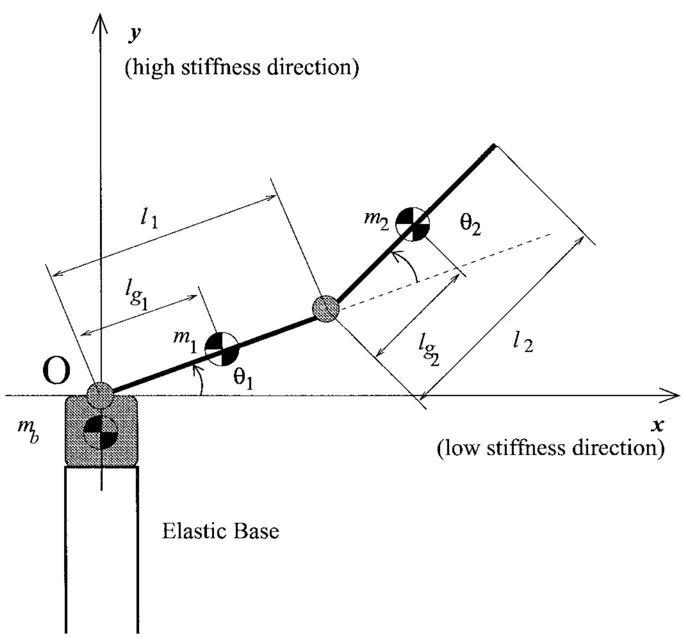

Fig. 7. The model of TREP.

motors $(n = 2)$, the (selective) reaction null space is one-dimensional, meaning that there is one nonzero vector in the reaction null space. The inertia coupling matrix of this model can be determined from the equation for the velocity of the

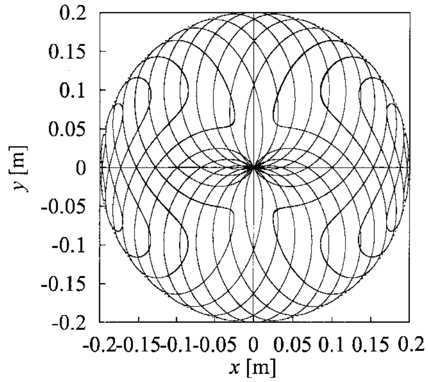

Fig. 8. Reactionless paths in the workspace of TREP.

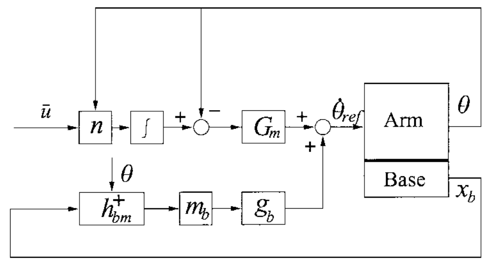

Fig. 9. Experimental controller block diagram.

manipulator center of mass, projected onto the low-stiffness axis. This is written as

$$w\dot{r}^x_{cm} = \boldsymbol{h}_{bm}\begin{bmatrix}\dot{\theta}_1\\ \dot{\theta}_2\end{bmatrix} = \mathcal{L} \tag{26}$$

where $1 = m_1 + m_2$ denotes the total mass of the manipulator, and $\boldsymbol{h}_{bm} = [h_{bm1} \quad h_{bm2}]$ stands for the inertia coupling matrix, with

$$h_{bm1} = -(m_1 l_{g1} + m_2 l_1)\ \sin(\theta_1) - m_2 l_{g2}\ \sin(\theta_1 + \theta_2),$$
$$h_{bm2} = -m_2 l_{g2}\ \sin(\theta_1 + \theta_2).$$

The reaction null space vector becomes then

$$\boldsymbol{n} = [h_{bm2} \quad -h_{bm1}]^T. \tag{27}$$

Zero initial coupling momentum will be conserved with any joint velocity along the reaction null space vector. This vector induces a one-dimensional distribution in joint space, which is always integrable. Consequently, the set of reactionless paths of the system can be obtained. This set is displayed in Fig. 8.

C. Control Law Derivation

The derivation of the composite control law follows that presented in Section IV. More specifically, we will use the acceleration-based formulation which is most suitable for motor drivers admitting velocity commands, as is the case with TREP.

Equation (6) assumes the form

$$m_b\ddot{x}_b + k_b x_b + \dot{\boldsymbol{h}}_{bm}\dot{\boldsymbol{\theta}} = -\boldsymbol{h}_{bm}\ddot{\boldsymbol{\theta}} \tag{28}$$

where x_b denotes the deflection of the base from its equilibrium point. The control law (15) is written as

$$\ddot{\boldsymbol{\theta}} = \boldsymbol{h}^+_{bm}(m_b g_b \dot{x}_b - \dot{\boldsymbol{h}}_{bm}\dot{\boldsymbol{\theta}}) + \boldsymbol{n}u - \boldsymbol{G}_m\dot{\boldsymbol{\theta}} \tag{29}$$

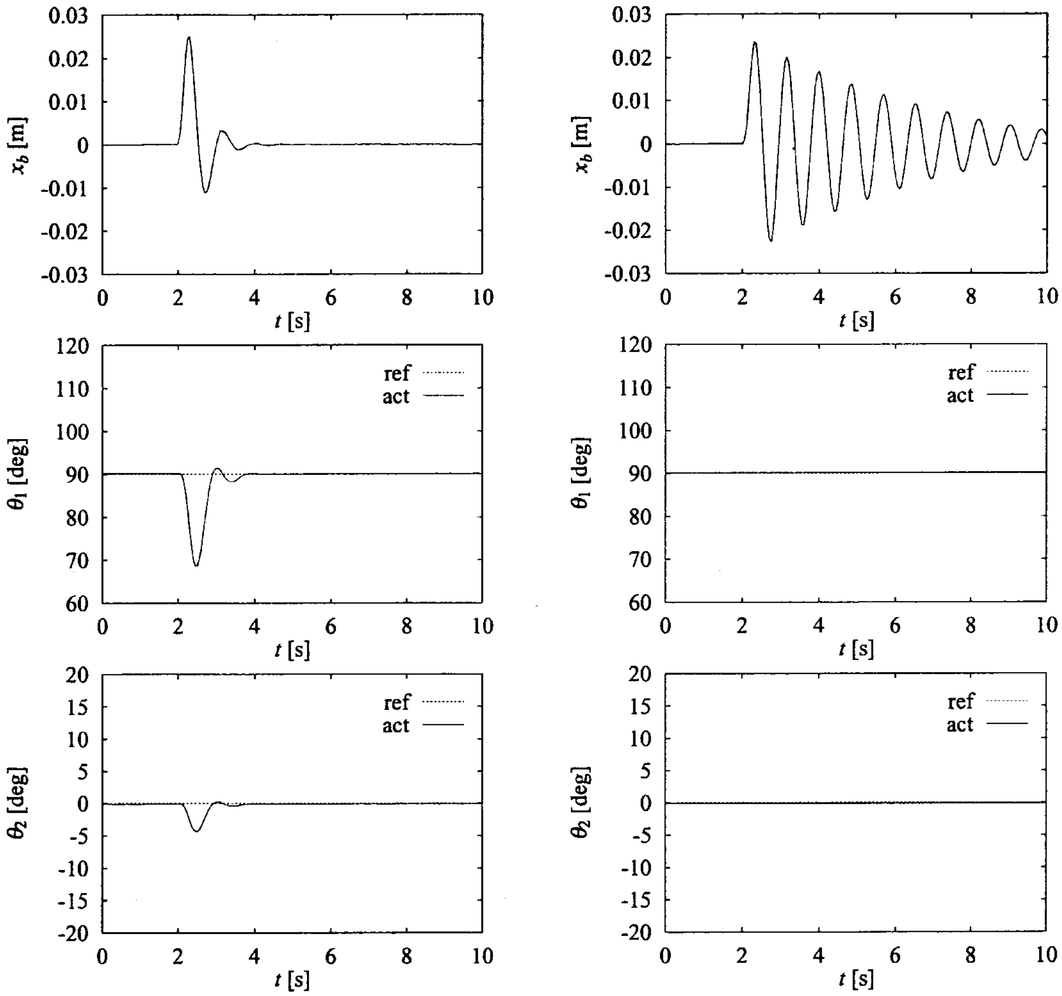

(a) (b)

Fig. 10. Base vibration: (a) with vibration suppression and (b) without vibration suppression (experiment).

where u is the additional control input. Because of the orthogonality between the two terms $\boldsymbol{h}_{bm}^{+}(\bullet)$ and $\boldsymbol{n}u$, it is clear that they will not influence each other. The pseudoinverse $\boldsymbol{h}_{bm}^{+}$ ensures the most efficient (in a least-squares sense) inertial coupling between the base and the manipulator.

The fact that the reaction null space is one-dimensional shows that there is only one degree-of-freedom left for the end-point control. This degree-of-freedom is realized as any desired (scalar) acceleration along the reactionless path. In practice this means that even very high velocity/acceleration would be admissible, as long as the motion does not deviate from the current reactionless path.

To adjust the composite control (29) to velocity command based motor drivers, we integrate the control. Thereby we assume that the rate of change of $\boldsymbol{h}_{bm}(\boldsymbol{\theta})$ is much slower then the rate of change of $\dot{x}_b$ which is justified if one considers the fact that x_b can be regarded as a "fast" variable. Thus, when integrating the term $\boldsymbol{h}_{bm}^{+} m_b g_b \dot{x}_b$ we assume a constant $\boldsymbol{h}_{bm}^{+}$, and obtain the following approximate integral form of the composite control (29):

$$\dot{\boldsymbol{\theta}} = \boldsymbol{h}_{bm}^{+} m_b g_b x_b + \boldsymbol{G}_m \left(\int \boldsymbol{n}\overline{u}\, dt - \boldsymbol{\theta} \right) \tag{30}$$

where $\boldsymbol{G}_m = g_m \boldsymbol{E}$, $g_m > 0$, $\overline{u} = u/g_m$. It is apparent that the reference reactionless path (determined by the integral in (30)) is tracked under position feedback control, making use of the gain g_m. Note that such representation was possible, since $\overline{u}$ can be chosen arbitrarily. A block diagram of the controller is shown in Fig. 9.

D. Experiments

We have conducted a series of experiments for vibration suppression, reactionless path tracking and composite control. In all the experiments, the initial configuration was the same: the arm was extended and aligned with the flexible base $(\theta_1 \cdot 90^\circ, \theta_2 \cdot 0)$.

1) Vibration Suppression: This experiment was performed at a fixed configuration, coinciding with the initial configuration mentioned above. The control law (30) was used, where the integral was replaced by the joint angles values of the fixed configuration. A relatively small position control gain was selected: $g_m = 20$ s^{-1}. The vibration gain was chosen as $g_b = 24$ s^{-1}. An arbitrary external force input was applied. Fig. 10(a) and (b) show the results for the cases with and without vibration suppression, respectively. The effectiveness of the vibration suppression was confirmed.

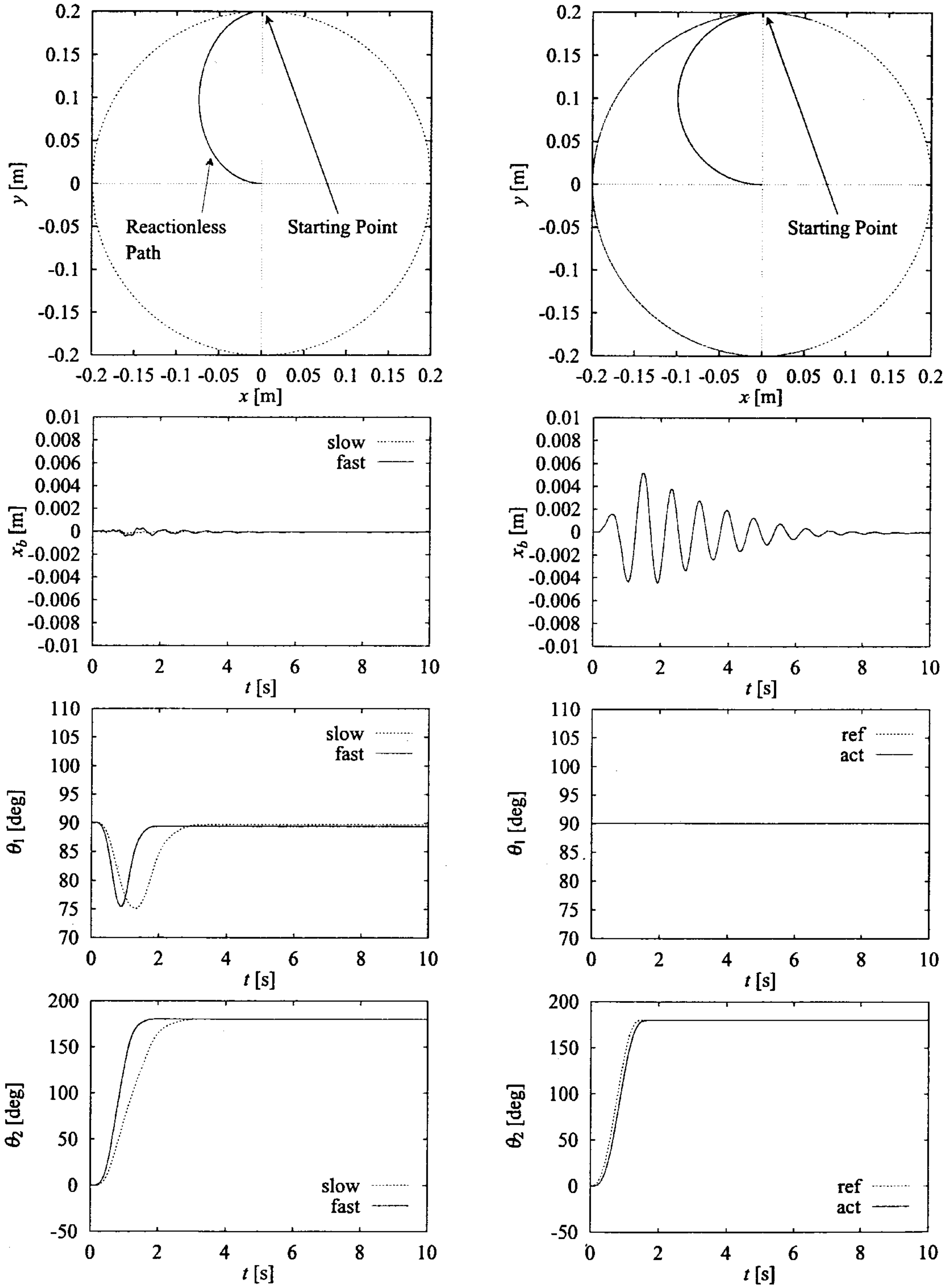

(a) (b)

Fig. 11. Path motion: (a) reactionless and (b) link 2 only (experiment).

2) Reactionless Motion: The same vibration suppression feedback gain was used ($g_b = 24\ \mathrm{s}^{-1}$). The position feedback gain was increased to $g_m = 50\ \mathrm{s}^{-1}$. The reactionless end-point reference path is shown in the upper part of Fig. 11(a). This path is generated on-line, by the integral term $\int \boldsymbol{n}\overline{u}\, dt$ in (30). The speed along the path was determined from the variable $\overline{u}$, which was designed as a fifth-order spline function of time. In order to verify the possibility for an arbitrary choice of $\overline{u}$, we performed the motion on the same path twice, with different velocities (called fast and slow). The lower three graphs in Fig. 11(a) show the results. It is seen that almost no base vibration is excited in both cases, in spite of the significant difference in the joint velocity. For comparison, Fig. 11(b) shows a point-to-point motion path with the same boundary conditions as in the previous motion. The base vibrates significantly.

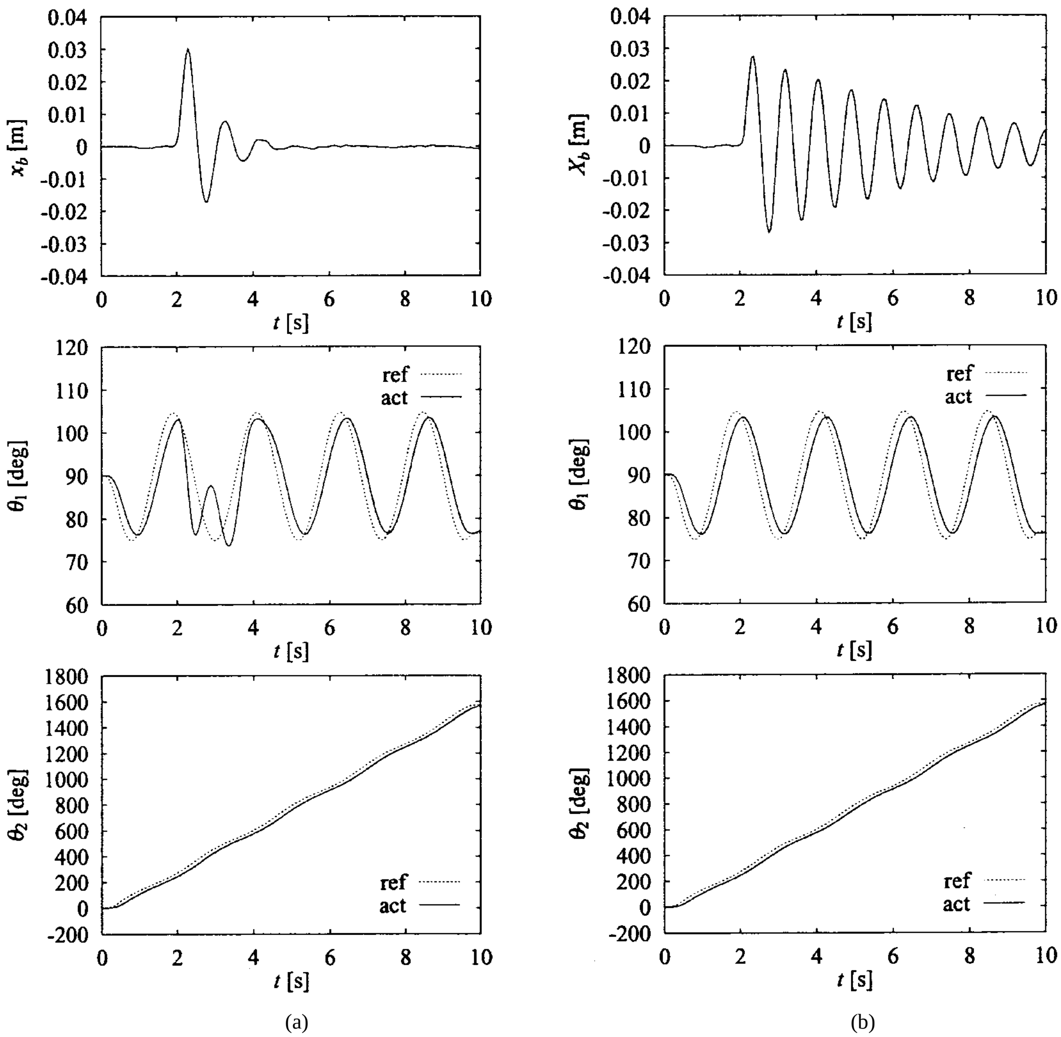

Fig. 12. Reactionless motion and base vibration: (a) with vibration suppression and (b) without vibration suppression (experiment).

TABLE I
MANIPULATOR LINK PARAMETERS OF TREP

l_1	0.1	[m]
l_2	0.1	[m]
lg_1	0.096	[m]
lg_2	0.090	[m]
m_1	0.310	[kg]
m_2	0.120	[kg]

TABLE II
FLEXIBLE BASE PARAMETERS OF TREP

length	0.5	[m]
hight	0.08	[m]
thickness	0.0007	[m]
beam interval	0.1	[m]
tip mass m_b	0.795	[kg]
stiffness k_b	77.9218	[N/m]

3) Control Experiment in the Presence of Unmodeled Dynamics: The above experiments have confirmed that the composite control law is useful to solve the vibration suppression task and the reactionless path tracking task *independently*. As already mentioned, we may expect that the control will be also useful when there is additional coupling resulting from simultaneous base vibration *and* manipulator motion.

The same reference reactionless path as in the previous experiment was used, which was tracked however in a cyclic manner. After accelerating the arm smoothly, the variable $\overline{u}$ was kept constant as $\overline{u} = 30$. While tracking, an external force was applied to the system. Fig. 12(a) and (b) display the results in the case with and without vibration suppression control, respectively. In the former case, we see that base vibration is effectively suppressed. Though, a comparison with the case when the initial state of the manipulator was stationary [cf. the upper part of Fig. 10(a)], shows slight deterioration in suppression performance. Of course, the arm deviates from the reactionless path when suppressing the vibration, but thereafter, it quickly converges to the reference input. No instability is observed. In the other case [Fig. 12(b)], by comparison with the upper part of Fig. 10(b), it is clearly seen that the vibration of the base is not disturbed at all through the reactionless joint motion.

VIII. Conclusion

The main contribution of this work are two composite control laws—one acceleration based, the other torque based—both of them capable of end-effector path tracking control without inducing disturbances on the flexible base, and in addition, of base vibration suppression control. Note that these are control subtasks two and one, respectively, as identified in the introduction. Some of the dynamic terms, e.g. nonlinear velocity-dependent coupling terms and dependencies of inertias on the elastic coordinates, have been ignored. Thus, complexity has been decreased, and we obtained controls which we claim to be suitable for real-time implementation, even in the case of larger systems. Besides decreased complexity there is another merit: the control gains can be selected in a straightforward manner since the manipulator and the flexible base are considered as two independent subsystems. Such independence is due to the orthogonal decomposition of joint space via the reaction null space operator. On the other hand, note that the independence means that, at least theoretically, the two subtasks cannot be tackled simultaneously. Experiments have shown, however, that system stability ensured via the reaction null space decomposition seems to have a sufficiently large margin to cope with the unmodeled nonlinear dynamic effects mentioned above, and hence, to ensure simultaneous subtask performance. The derivation of precise expressions for this stability margin is a matter of future studies. Note that such simultaneous subtask performance means that the controls can handle the third subtask identified in the introduction, as well.

The control laws proposed here are general enough to cover various cases of redundancy, including kinematic and dynamic redundancy, as well as redundancy due to selectivity, as introduced here. We have demonstrated via examples how the cases of kinematic redundancy and selective redundancy can be handled. Meanwhile, we were able to tackle also the case of dynamic redundancy, by adding a second arm to the experimental testbed TREP. The results obtained [27] agree well with the theories presented here.

Finally, we note that the decomposition of the dynamics by means of the inertia coupling matrix, as well as the analysis based on the coupling momentum, provides insight into the physics of the system. For example, it shows clearly that base vibration suppression in a system without energy dissipation results in change of the coupling momentum, such that after the suppression the manipulator never comes to rest.

Acknowledgment

The authors would like to thank Dr. A. Konno, K. Abe, T. Miwa, and S. Okada for their help in designing TREP.

References

[1] A. Sharon and D. Hardt, "Enhancement of robot accuracy using end-point feedback and a macro-micro manipulator system," in *Proc. ACC*, San Diego, CA, 1984, pp. 1836–1842.
[2] J. F. Jansen *et al.*, "Long-reach manipulation for waste storage tank remediation," *ASME J.*, vol. 31, pp. 67–73, 1991.
[3] D.-S. Kwon *et al.*, "Input shaping filter methods for the control of structurally flexible, long-reach manipulators," in *Proc. IEEE Int. Conf. Robot. Automat.*, San Diego, CA, 1994, pp. 3259–3264.
[4] M. A. Torres and S. Dubowsky, "Path-planning in elastically constrained space manipulator systems," in *Proc. IEEE Int. Conf. Robot. Automat.*, Atlanta, GA, 1993, pp. 812–817.
[5] C. Vallancourt and C. M. Gosselin, "Compensating for the structural flexibility of the SSRMS with the SPDM," in *Proc. 2nd Workshop Robot. Space*, Canadian Space Agency, Montreal, PQ, Canada, July 1994.
[6] T. Yoshikawa *et al.*, "Quasistatic trajectory tracking control of flexible manipulator by macro-micro manipulator system," in *Proc. 1993 IEEE Int. Conf. Robot. Automat.*, Atlanta, GA, May 1993, pp. 210–215.
[7] ——, "Dynamic trajectory tracking control of flexible manipulator by macro-micro manipulator system," in *Proc. 1994 IEEE Int. Conf. Robot. Automat.*, San Diego, CA, May 1994, pp. 1804–1809.
[8] W. Yim and S. N. Singh, "Nonlinear inverse and predictive end point trajectory control of flexible macro-micro manipulators," *Trans. ASME, J. Dyn. Syst., Meas. Contr.*, vol. 119, pp. 412–420, Sept. 1997.
[9] S. H. Lee and W. J. Book, "Robot vibration control using inertial damping forces," in *Proc. 8th CISM–IFToMM Symp. RoManSy 8*, Cracow, Poland, 1990, pp. 252–259.
[10] M. A. Torres, S. Dubowsky, and A. C. Pisoni, "Vibration control of deployment structures' long-reach manipulators: The P-PED method," in *Proc. 1996 IEEE Int. Conf. Robot. Automat.*, Minneapolis, MN, Apr. 1996, pp. 2498–2504.
[11] J. Y. Lew and D. J. Trudnowski, "Vibration control of a micro/macro manipulator system," *IEEE Contr. Syst. Mag.*, vol. 16, no. 1, pp. 26–31, Feb. 1996.
[12] I. Sharf, "Active damping of a large flexible manipulator with a short-reach robot," *Trans. ASME, J. Dyn. Syst., Meas. Contr.*, vol. 118, pp. 704–713, Dec. 1996.
[13] D. W. Cannon *et al.*, "Experimental study on micro/macro manipulator vibration control," in *Proc. IEEE Int. Conf. Robot. Automat.*, Minneapolis, MN, 1996, pp. 2549–2554.
[14] R. H. Cannon, Jr. and E. Schmitz," Initial experiments on the end-point control of a flexible one-link robot," *Int. J. Robot. Res.*, vol. 3, no. 3, pp. 62–75, 1984.
[15] C. Mavroidis, S. Dubowsky, and V. Raju, "End-point control of long reach manipulator systems," in *Proc. 9th World Congr. IFToMM*, Milano, Italy, 1995, pp. 1740–1744.
[16] M. L. Hanson and R. H. Tolson, "Reducing flexible base vibrations through local redundancy resolution," *J. Robot. Syst.*, vol. 12, no. 11, pp. 767–779, 1995.
[17] T. Arai *et al.*, "Proposal of dynamic redundancy in robot control," in *Proc. IEEE/RSJ Int. Workshop Intell. Robots Syst. (IROS'92)*, Raleigh, NC, 1992, pp. 1921–1926.
[18] D. N. Nenchev, K. Yoshida, and Y. Umetani, "Analysis, design and control of free-flying space robots using fixed-attitude-restricted Jacobian matrix," *Robotics Research: The Fifth International Symposium*, H. Miura and S. Arimoto, Eds. Cambridge, MA: MIT Press, 1990, pp. 251–258.
[19] D. N. Nenchev, Y. Umetani, and K. Yoshida, "Analysis of a redundant free-flying spacecraft/manipulator system," *IEEE Trans. Robot. Automat.*, vol. 8, pp. 1–6, Feb. 1992.
[20] D. N. Nenchev, "A controller for a redundant free-flying space robot with spacecraft attitude/manipulator motion coordination," in *Proc. 1993 IEEE/RSJ Int. Conf. Intell. Robots Syst. (IROS'93)*, Yokohama, Japan, 1993, pp. 2108–2114.
[21] A. Konno *et al.*, "Configuration-dependent vibration controllability of flexible-link manipulators," *Int. J. Robot. Res.*, vol. 16, no. 4, pp. 567–576, 1997.
[22] K. Yoshida, D. N. Nenchev, and M. Uchiyama, "Moving base robotics and reaction management control," *Robotics Research: The Seventh International Symposium*, G. Giralt and G. Hirzinger, Eds. New York: Springer-Verlag, 1996, pp. 101–109.

[23] K. Yoshida and D. N. Nenchev, "A general formulation of under-actuated manipulator systems," in *Preprints 8th Int. Symp. Robotics Research*, Hayama, Japan, 1997, pp. 72–79.
[24] D. N. Nenchev, K. Yoshida, and M. Uchiyama, "Reaction null-space based control of flexible structure mounted manipulating systems," in *Proc. 35th IEEE CDC*, Kobe, Japan, 1996, pp. 4118–4123.
[25] A. Isidori, *Nonlinear Control Systems*, 3rd ed. New York: Springer-Verlag, 1995.
[26] D. N. Nenchev, "Restricted Jacobian matrices of redundant manipulators in constrained motion tasks," *Int. J. Robot. Res.*, vol. 11, no. 6, pp. 584–597, 1993.
[27] A. Gouo *et al.*, "Dual-arm long-reach manipulators: Noncontact motion control startegies," in *Proc. IEEE/RSJ Int. Conf. Intell. Robots Syst. (IROS'98)*, Victoria, B.C., Canada, Oct. 1998, pp. 449–454.

Dragomir N. Nenchev (M'92) received the B.Eng. degree in computer science, the M.Eng. degree, and the Ph.D. degree in robotics, all from the Higher Institute of Electrical and Mechanical Engineering (now Technical University), Sofia, Bulgaria in 1979, 1981, and 1985, respectively.

He has been with the Robotics Department, Technical University of Sofia, and with the Department of Aeronautics and Space Engineering, Tohoku University, Sendai, Japan, and the Department of Mechanical and Production Engineering, Niigata University, Japan. He is now Professor with the Department of Intelligent Machines and System Engineering, Hirosaki University, Hirosaki, Japan. He was also a Visiting Researcher with the Department of Mechanical Engineering Science, Tokyo Institute of Technology, Tokyo, Japan, from 1988 to 1989, and the Department of Mechanics, Milan Polytechnic, Italy, from 1992 to 1993. His research interests are in kinematics, dynamics and motion control of underactuated, parallel, and redundant robot systems.

Kazuya Yoshida (M'91) received the B.Eng., M.Eng., and Dr.Eng. degrees from the Tokyo Institute of Technology, Tokyo, Japan, in 1984, 1986 and 1990, respectively.

From 1986 to 1994, he was with Department of Mechanical Engineering of Science (Mechano-Aerospace), Tokyo Institute of Technology, Tokyo, as a Research Associate. During this period, he stayed with the Swiss Federal Institute of Technology (ETH) in September 1993, and with the Massachusetts Institute of Technology (MIT), Cambridge, from March 1994 to March 1995, as a Visiting Scientist. Since 1995 he has been an Associate Professor in the Department of Aeronautics and Space Engineering, Tohoku University, Sendai, Japan. His current interests include the dynamics and control of both free-flying and elastically mounted space manipulators, and the design and dynamic analysis of planetary exploration robots.

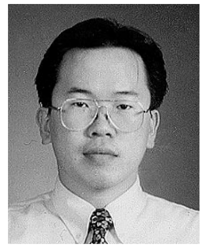

Prasert Vichitkulsavat received the B.Eng. and M.Eng. degrees from Tohoku University, Sendai, Japan, in 1994 and 1996, respectively. The research work presented in this paper was performed as his M.Eng. thesis.

He was with Siam-Hitachi Elevator Co., Ltd., and Thai Ikeda Mfg. Co., Ltd., and T. Nongkarm A. Sriracha Chonburi, Thailand.

Masaru Uchiyama (M'79) received the B.Eng., M.Eng., and Ph.D. degrees from the University of Tokyo, Tokyo, Japan, in 1972, 1974, and 1977, respectively, all in mechanical engineering.

Since 1977, he has been with the School of Engineering, Tohoku University, Sendai, Japan and currently is a Professor of the Spacecraft Systems Laboratory, Department of Aeronautics and Space Engineering. He was a Visiting Fellow at the University of Newcastle upon Tyne, U.K., from 1982 to 1983, and a Visiting Professor at the University of California, Santa Barbara, from 1986 to 1987. Currently he is a Visiting Professor at the Institute of Space and Astronautical Science, Japan, since April 1999. His research interests are manipulation robotics and its application to aerospace engineering.